# Highly efficient lasing and thermal properties of Tm:Y2O3 and Tm:(Y,Sc)2O3 ceramics

Kirill Eremeev, Pavel Loiko, Roman Maksimov, Vladislav Shitov, Vladimir Osipov, Dmitry Vakalov, Viacheslav Lapin, Patrice Camy, Weidong Chen, Uwe Griebner, et al.

# Highly efficient lasing and thermal properties of $Tm:Y_2O_3$ and $Tm:(Y,Sc)_2O_3$ ceramics

KIRILL EREMEEV,[1] PAVEL LOIKO,[1] ROMAN MAKSIMOV,[2,3] VLADISLAV SHITOV,[2] VLADIMIR OSIPOV,[2] DMITRY VAKALOV,[4] VIACHESLAV LAPIN,[4] PATRICE CAMY,[1] WEIDONG CHEN,[5] UWE GRIEBNER,[5] VALENTIN PETROV,[5] AND ALAIN BRAUD[1,*]

[1]*Centre de Recherche sur les Ions, les Matériaux et la Photonique (CIMAP), UMR 6252 CEA-CNRS-ENSICAEN, Université de Caen, 6 Boulevard Maréchal Juin, 14050 Caen Cedex 4, France*
[2]*Institute of Electrophysics, Ural Branch of the Russian Academy of Sciences, 106 Amundsen St., 620016 Ekaterinburg, Russia*
[3]*Ural Federal University named after the first President of Russia B. N. Yeltsin, 19 Mira St., 620002 Ekaterinburg, Russia*
[4]*North-Caucasus Federal University, 2 Kulakova Ave., 355017 Stavropol, Russia*
[5]*Max Born Institute for Nonlinear Optics and Short Pulse Spectroscopy, Max-Born-Str. 2a, D-12489 Berlin, Germany*
**Corresponding author: alain.braud@ensicaen.fr*

Received XX Month XXXX; revised XX Month, XXXX; accepted XX Month XXXX; posted XX Month XXXX (Doc. ID XXXXX); published XX Month XXXX

**We report on thermal, spectroscopic and laser properties of transparent 5 at.% $Tm^{3+}$-doped yttria and "mixed" yttria-scandia ceramics fabricated by vacuum sintering at 1750 °C using nanoparticles produced by laser ablation. The solid-solution $(Tm_{0.05}Y_{0.698}Sc_{0.252})_2O_3$ ceramic features a broadband emission extending up to 2.3 μm (gain bandwidth: 167 nm) and high thermal conductivity of 4.48 $Wm^{-1}K^{-1}$. A $Tm:Y_2O_3$ ceramic laser generated 812 mW at 2.05 μm with a slope efficiency $\eta$ of 70.2%. For the $Tm:(Y,Sc)_2O_3$ ceramic, the output power was 523 mW at 2.09 μm with $\eta$ = 44.7%. These results represent record-high slope efficiencies for any parent or "mixed" $Tm^{3+}$-doped sesquioxide ceramics. © 2023 Optical Society of America**

http://dx.doi.org/10.1364/OL.99.099999

Thulium ions ($Tm^{3+}$, electronic configuration: $[Xe]4f^{12}$) are known for their broadband emission in the eye-safe spectral range around 2 μm due to the $^3F_4 \rightarrow {}^3H_6$ electronic transition [1]. $Tm^{3+}$ ions offer intense absorption at 0.8 μm (the spectral range covered by AlGaAs diode lasers) and a cross-relaxation (CR) process, $^3H_4 + {}^3H_6 \rightarrow {}^3F_4 + {}^3F_4$, leading to a pump quantum efficiency up to 2 (a one-to-two pump process) [2]. Due to the large Stark splitting of the ground-state ($^3H_6$, 788 $cm^{-1}$ for $Tm:Y_2O_3$ [3]), $Tm^{3+}$-doped crystals are extremely suitable for broadly tunable and mode-locked lasers [4,5].

Among the host matrices for $Tm^{3+}$ doping, cubic (sp. gr. $Ia\bar{3}$, C-type) rare-earth sesquioxides $A_2O_3$ (A = Y, Lu, Sc) appear attractive because of a combination of good thermal conductivity of the host matrix ($\kappa$ = 12.7 $Wm^{-1}K^{-1}$ for $Y_2O_3$) and advantageous spectroscopic properties of the dopant ions, i.e., broad emission spectra extending well above 2 μm owing to strong crystal-fields, long upper laser level luminescence lifetimes and efficient CR [1]. Highly-efficient and power-scalable $Tm:A_2O_3$ lasers at ~2 μm are known [1,6,7]. Loiko *et al.* reported on a diode-pumped $Tm:Lu_2O_3$ crystal-rod laser generating 47.5 W at 2.1 μm with a slope efficiency of 59% [1]. However, the growth of $Tm:A_2O_3$ single-crystals is complicated by their high melting points (2425 °C for $Y_2O_3$) which are withstood only by Rh crucibles [8].

Transparent ceramics are polycrystalline materials composed of closely packed single-crystalline grains with a random orientation featuring a weak light scattering under a low density of pores and a lack of secondary phases. The ceramic technology is well applicable to cubic sesquioxides [7,9,10] offering lower synthesis temperature (~1750 °C), well-preserved spectroscopic behavior of the dopant ions, good thermo-mechanical properties (under proper synthesis conditions) and well-controlled doping. $Tm:A_2O_3$ laser ceramics are known [7,11-13]. Wang *et al.* reported on a diode-pumped 2 at.% $Tm:Y_2O_3$ ceramic laser delivering 7.25 W at 2.05 μm with a slope efficiency of 40% exceeding the Stokes limit [13].

Apart from the parent sesquioxides, their binary solid-solutions $Tm:(A_{1-x}B_x)_2O_3$ attract attention for generation of ultrashort pulses from mode-locked lasers [5,14]. This is due to an inhomogeneous spectral broadening in such compounds. Zhao *et al.* reported on a mode-locked $Tm:LuYO_3$ ceramic laser delivering pulses as short as 57 fs at 2045 nm, i.e., 8 optical cycles [5]. The ceramic technology is suited for the precise control of the A/B balances in such materials.

In the present work, we report on the thermal and spectroscopic properties and highly-efficient ~2 μm laser operation of $Tm:Y_2O_3$ and $Tm:(Y,Sc)_2O_3$ transparent sesquioxide ceramics fabricated by an original method employing laser-ablated nanoparticles.

Transparent $Tm:(Y_{1-x}Sc_x)_2O_3$ ceramics were fabricated by solid-state consolidation of nanoparticles synthesized by laser ablation of a solid target material [15]. To prepare the targets, commercial high-purity $A_2O_3$ (A = Y, Sc, Tm) powders were dry-mixed for 24 h in the proportion $Tm_{0.05}(Y_{1-x}Sc_x)_{1.95}O_3$ ($x$ = 0, 0.125, 0.25). A small amount of $ZrO_2$ (1.7 mol%) acting as a grain growth inhibitor was used [16]. The mixtures were compacted and sintered at 1100 °C for 5 h in air. The vapor phase above the target surface formed under irradiation by a pulsed $CO_2$ laser was cooled by an air flow to condense and crystallize as nanoparticles. Their composition was $(Tm_{0.05}Y_{0.95})_2O_3$, $(Tm_{0.05}Y_{0.829}Sc_{0.121})_2O_3$ and $(Tm_{0.05}Y_{0.698}Sc_{0.252})_2O_3$ according to the ICP-MS analysis. They were calcined at 1050 °C and

uniaxially pressed in a stainless-steel die at 200 MPa to form green bodies, which were sintered at 1750 °C for 5 h under a residual gas pressure of $10^{-3}$ Pa. The sintered ceramics were annealed at 1400 °C for 2 h in air. The ceramic disks (Φ12 mm, ~1.8-1.9 mm-thick) were polished to laser-grade quality on both sides. A photograph of annealed polished ceramic disks is shown in Fig. 1(a). They were transparent with a slight yellow coloration due to $Tm^{3+}$ doping.

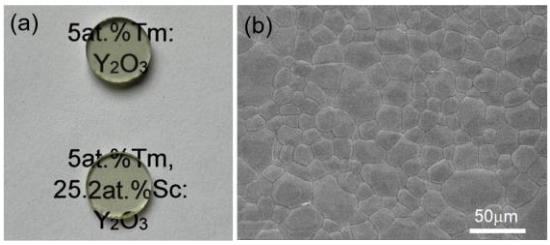


**Fig. 1.** 5 at.% Tm:$(Y_{1-x}Sc_x)_2O_3$ ceramics: (a) a photograph of laser-grade polished ceramic disks; (b) a typical SEM image of an etched surface of the $(Tm_{0.05}Y_{0.829}Sc_{0.121})_2O_3$ ceramic.

The ceramics were of single-phase nature (sp. gr. $Ia\bar{3}$, bixbyite structure). A typical SEM image of a thermally etched surface of the $(Tm_{0.05}Y_{0.829}Sc_{0.121})_2O_3$ ceramic is shown in Fig. 1(b). The samples consisted of polyhedral-shaped micro-crystallites separated by well-defined and clean boundaries. Partial substitution of $Y^{3+}$ by $Sc^{3+}$ accelerated the diffusion processes and caused a notable increase in the grain size ($D_{grain}$ = 6.8, 21.2 and 28.2 μm for 0, 12.1 and 25.2 at.% $Sc^{3+}$). The content of μm-sized pores progressively increased, $X_{pore}$ = 0.6, 25.9 and 46.1 ppm, respectively. It is likely that the accelerated grain growth led to entrapment of a considerable fraction of pores. The transmission of the ceramic disks at ~1 μm was $T$ = 81.5%, 81.0% and 80.5%, respectively, close to the theoretical limit.

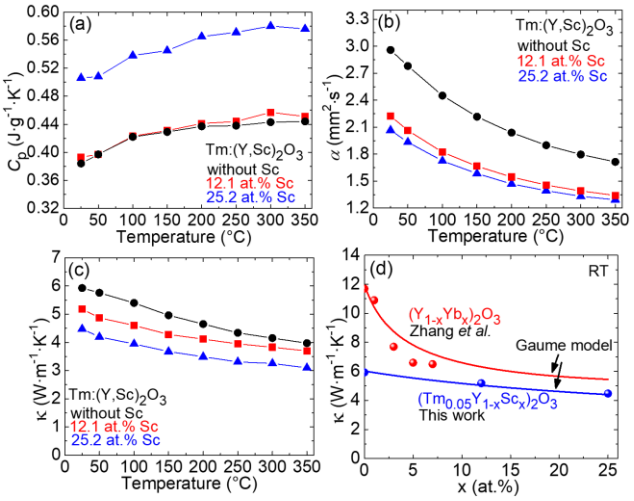


**Fig. 2.** 5 at.% Tm:$(Y_{1-x}Sc_x)_2O_3$ ceramics: temperature dependence of (a) specific heat $C_p$, (b) thermal diffusivity $\alpha$ and (c) thermal conductivity $\kappa$; (d) RT thermal conductivity for $(Tm_{0.05}Y_{1-x}Sc_x)_2O_3$ and $(Y_{1-x}Yb_x)_2O_3$ [17] ceramics, *points* – experiment, *curves* – simulation (Gaume model).

The thermophysical characteristics of ceramics were studied by the laser flash method using a NETZSCH LFA 467 HyperFlash at 25 – 350 °C under Ar atmosphere. The samples were covered with a graphite layer. The thermal conductivity was calculated as $\kappa = \alpha C_p \rho$, where $\alpha$ is the thermal diffusivity, $C_p$ is the specific heat and $\rho$ is the density evaluated from the XRD analysis, see Fig. 2(a-c). At room temperature (RT), $\kappa$ gradually decreases from 5.93 to 4.48 $Wm^{-1}K^{-1}$ when raising the $Sc^{3+}$ content from 0 to 25.2 at.%. The concentration dependence of $\kappa$ for $(Tm_{0.05}Y_{1-x}Sc_x)_2O_3$ and $(Y_{1-x}Yb_x)_2O_3$ [17] ceramics is well explained using the Gaume model [18], Fig. 2(d).

The formation of a substitutional solid-solution for Sc-containing ceramics was confirmed by Raman spectroscopy, Fig. 3. The most intense Raman band assigned to $F_g + A_g$ modes of the cubic bixbyite structure broadens and experiences a progressive shift towards higher frequencies with increasing the $Sc^{3+}$ content. For 25.2 at.% $Sc^{3+}$, it is centered at 390 $cm^{-1}$ (bandwidth: 31 $cm^{-1}$) and the highest phonon energy is 614 $cm^{-1}$.

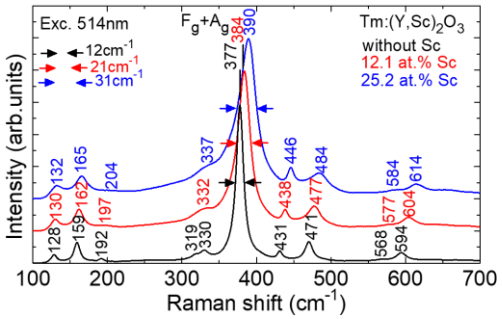


**Fig. 3.** Raman spectra of 5 at.% Tm:$(Y_{1-x}Sc_x)_2O_3$ ceramics, $\lambda_{exc}$ = 514 nm, *numbers* – Raman frequencies in $cm^{-1}$.

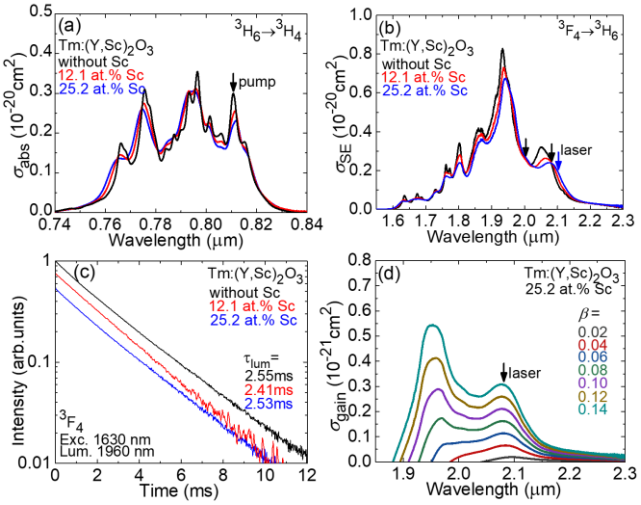


**Fig. 4.** Spectroscopy of $Tm^{3+}$ ions in $(Y_{1-x}Sc_x)_2O_3$ ceramics ($x$ = 0 – 0.252): (a) absorption cross-sections, $\sigma_{abs}$, for the $^3H_6 \rightarrow {}^3H_4$ transition; (b) SE cross-sections, $\sigma_{SE}$, for the $^3F_4 \rightarrow {}^3H_6$ transition; (c) luminescence decay curves from the $^3F_4$ manifold, $\lambda_{exc}$ = 1630 nm, $\lambda_{lum}$ = 1960 nm, powdered samples, $\tau_{lum}$ – luminescence lifetime; (d) gain cross-sections, $\sigma_{gain} = \beta\sigma_{SE} - (1-\beta)\sigma_{abs}$, $\beta = N_2(^3F_4)/N_{Tm}$ - inversion ratio. *Arrows* indicate the pump and laser wavelengths.

Figure 4(a) shows the absorption cross-sections, $\sigma_{abs}$, for the $^3H_6 \rightarrow {}^3H_4$ $Tm^{3+}$ transition. The $Tm^{3+}$ ion density $N_{Tm}$ was 1.35, 1.38 and

1.42 [$10^{21}$ at/cm$^3$] for 0, 12.1 and 25.2 at.% $Sc^{3+}$, respectively. By adding $Sc^{3+}$, the absorption spectra become less structured. For the $(Tm_{0.05}Y_{0.698}Sc_{0.252})_2O_3$ ceramic, the maximum $\sigma_{abs}$ is $0.31\times10^{-20}$ cm$^2$ at 795.3 nm corresponding to an absorption bandwidth (FWHM) of 25 nm. The stimulated-emission (SE) cross-section spectra for the $^3F_4 \rightarrow {}^3H_6$ transition are plotted in Fig. 4(b). By replacing $Y^{3+}$ cations ($R_Y$ = 0.9 Å for VI-fold $O^{2-}$ coordination) with much smaller $Sc^{3+}$ ones ($R_{Sc}$ = 0.745 Å), the emission spectra of $Tm^{3+}$ ions broadened and shifted towards longer wavelengths due to increased crystal-field strength in scandia as compared to yttria. In the spectral range where laser operation is expected for the $(Tm_{0.05}Y_{0.698}Sc_{0.252})_2O_3$ ceramic, $\sigma_{SE} = 0.24\times10^{-20}$ cm$^2$ at 2075.6 nm. The reabsorption-free upper laser level ($^3F_4$) lifetime of $Tm^{3+}$ ions was weakly dependent on the $Sc^{3+}$ content, $\tau_{lum}$ = 2.41 – 2.55 ms, Fig. 4(c). The gain cross-sections, $\sigma_{gain} = \beta\sigma_{SE} - (1-\beta)\sigma_{abs}$, for the $^3F_4 \leftrightarrow {}^3H_6$ transition were calculated. For $(Tm_{0.05}Y_{0.698}Sc_{0.252})_2O_3$, for small inversion ratios $\beta$ < 0.06, a local peak at ~2.09 μm dominates in the spectra and for higher $\beta$, another peak at ~1.95 μm appears. For small $\beta$ = 0.06, the gain bandwidth (FWHM) reaches 167 nm indicating a great potential for ultrashort (sub-100 fs) pulse generation.

The inhomogeneous spectral broadening of $Tm^{3+}$ absorption / emission bands in "mixed" (solid-solution) ceramics was confirmed by low temperature (12 K) spectroscopy of the $^3F_4 \leftrightarrow {}^3H_6$ transition, Fig. 5. An additional spectral broadening as compared to Tm:$Y_2O_3$ single-crystals was induced by $ZrO_2$.

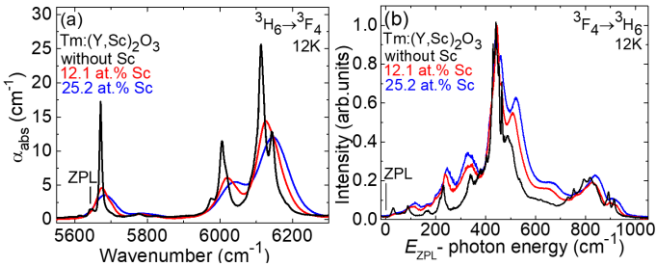


**Fig. 5.** Low-temperature (LT, 12 K) spectroscopy of $Tm^{3+}$ ions in the $Y_2O_3$ and $(Y,Sc)_2O_3$ ceramics: (a) the $^3H_6 \rightarrow {}^3F_4$ transition in absorption; (b) the $^3F_4 \rightarrow {}^3H_6$ transition in emission. ZPL – zero-phonon line.

For laser experiments, we employed the $(Tm_{0.05}Y_{0.698}Sc_{0.252})_2O_3$ and $(Tm_{0.05}Y_{0.95})_2O_3$ ceramics. The laser elements were cut from the central part of the ceramic disks, they were double-side polished to laser-grade quality with good parallelism and left uncoated. They were fixed on a passively cooled Cu-holder using a silver paint. A hemispherical cavity was formed by a flat pump mirror (PM) coated for high transmission (HT, $T$ = 78.7%) at 0.81 μm and high reflection (HR, $R$ > 99.9%) at 1.86 – 2.33 μm and a concave (radius of curvature: -100 mm) output coupler (OC) with a transmission $T_{OC}$ in the range of 0.2% - 3.5% at the laser wavelength. The total cavity length was 102 mm. The laser element was placed near the PM with an airgap of <1 mm. The pump source was a Ti:Sapphire laser (3900S, Spectra Physics) delivering up to 4.0 W at 811 nm with a nearly diffraction limited beam ($M^2 \sim 1$). The pump radiation was focused into the ceramic through the PM using an AR-coated aspherical lens (f = 75 mm). The pump spot diameter in the focus was 50±10 μm. The pumping was in double-pass due to a back-reflection from the OCs at the pump wavelength ($R$ ~80%). For the $(Tm_{0.05}Y_{0.95})_2O_3$ ceramic and the optimum $T_{OC}$ = 3.5%, the total pump absorption under lasing conditions was 51.0% representing certain ground-state ($^3H_6$) bleaching. The radius of the laser mode in the ceramic was calculated using the ABCD method accounting for the thermal lens in Tm:$Y_2O_3$, $w_L$ = 57±5 μm, indicating a good mode-matching. The spectra of laser emission were measured using an optical spectrum analyzer (Yokogawa, AQ6376).

The $(Tm_{0.05}Y_{0.95})_2O_3$ ceramic delivered a maximum output power of 812 mW with a high slope efficiency $\eta$ of 70.2% (vs. the absorbed pump power) for $T_{OC}$ = 3.5%, Fig. 6(a). With increasing the output coupling, the laser threshold gradually increased from 90 mW ($T_{OC}$ = 0.2%) to 393 mW ($T_{OC}$ = 3.5%). The emission wavelength experienced a slight blue-shift with increasing the output coupling, from 2061–2085 nm ($T_{OC}$ = 0.2%) to 2048–2063 nm ($T_{OC}$ = 3.5%) owing to the quasi-three-level nature of the $^3F_4 \rightarrow {}^3H_6$ transition with reabsorption, Fig. 6(c). The obtained laser slope efficiency exceeds the Stokes limit, $\eta_{StL} = \lambda_P/\lambda_L$ = 39.6%, owing to an efficient CR among adjacent $Tm^{3+}$ ions. After Loiko *et al.* [1], for 5 at.% $Tm^{3+}$ doping in $Y_2O_3$, the quantum efficiency of excitation into the $^3F_4$ manifold is $\eta_q$ = 1.97±0.03 (almost ideal one-to-two process). The upper limit for the slope efficiency is then [2] $\eta < \eta_{StL}\eta_q\eta_{mode}\eta_{OC}$ = 69±3%, where $\eta_{OC} = \ln[1 - T_{OC}]/\ln[(1 - T_{OC})(1 - L)]$ = 87±3% is the output-coupling efficiency ($L$ is the round-trip passive loss, see below) and $\eta_{mode} \approx 1$ is the mode-matching one.

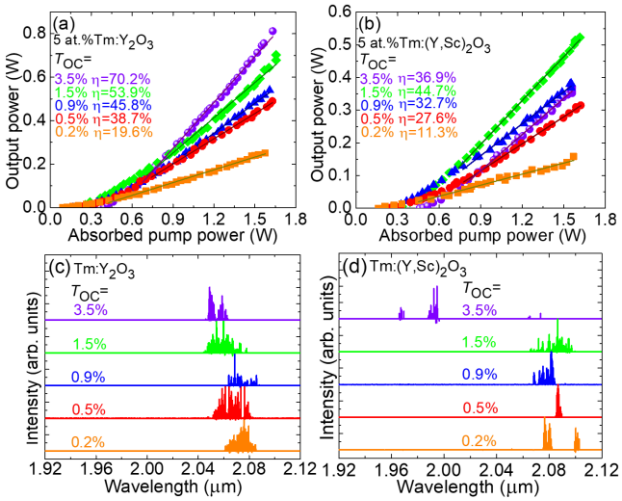


**Fig. 6.** ~2 μm laser performance of (a,c) $(Tm_{0.05}Y_{0.95})_2O_3$ and (b,d) $(Tm_{0.05}Y_{0.698}Sc_{0.252})_2O_3$ ceramics: (a,b) input-output dependences, $\eta$ – slope efficiency; (c,d) typical spectra of laser emission.

For the yttria-scandia $(Tm_{0.05}Y_{0.698}Sc_{0.252})_2O_3$ ceramic, the laser generated 523 mW at 2065 – 2097 nm with a lower $\eta$ of 44.7% and a laser threshold of 275 mW (for $T_{OC}$ = 1.5%), Fig. 6(c). The laser threshold was in the range 165 – 484 mW for output coupler transmissions between 0.3% and 3.5%. The lower slope efficiency for the Sc-containing ceramic is related to higher passive losses caused by the residual porosity. The laser emission spectra for the "mixed" ceramic are shown in Fig. 6(d). For $T_{OC} \le$ 1.5%, the laser operated at 2.08 μm and for higher output coupling, additional lines at 1.96 and 1.99 μm appeared. This behavior agrees with the gain spectra for increased inversion ratios, cf. Fig. 4(d). A clear red-shift of the laser wavelength due to the $Sc^{3+}$ effect on the emission spectra was observed.

The round-trip passive losses in the ceramics were evaluated using the Findlay-Clay analysis [19] by plotting the laser threshold

$P_{th}$ versus $\ln(1/R_{OC})$ where $R_{OC} = 1 - T_{OC}$ is the output coupler reflectivity, Fig. 7. This analysis yielded $L = 0.5\pm0.2\%$ and $1.5\pm0.3\%$ for the yttria and yttria-scandia ceramics, respectively. The increase in the passive losses for the Sc-containing ceramic agrees with the higher content of pores for this material.

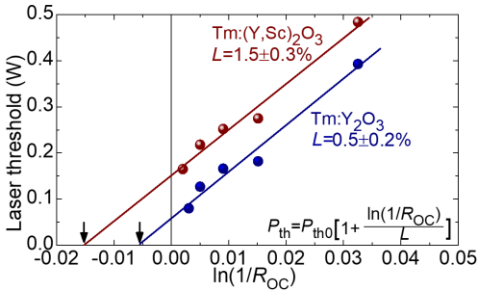


**Fig. 7.** The Findlay-Clay analysis for estimating the round-trip passive loss $L$ for $(Tm_{0.05}Y_{0.95})_2O_3$ and $(Tm_{0.05}Y_{0.698}Sc_{0.252})_2O_3$ ceramics.

Suzuki *et al.* studied $(Tm_{0.031}Y_{0.474}Sc_{0.495})_2O_3$ single-crystals grown by the Czochralski method at a reduced temperature of 2100 °C. Under diode-pumping at 780 nm, an output power of 422 mW was generated at 2.11 μm with $\eta$ = 45% [20]. Jing *et al.* reported on a diode-pumped $(Tm_{0.048}Lu_{0.635}Sc_{0.317})_2O_3$ ceramic laser delivering 1.01 W at 2.10 μm with lower $\eta$ = 24% [12]. Pirri *et al.* reported on a quasi-CW diode-pumped $(Tm_{0.05}Sc_{0.252}Y_{0.698})_2O_3$ ceramic laser generating 1.24 W at 2.08 μm with lower $\eta$ =9.5% [21]. Our results for the Tm:$(Y,Sc)_2O_3$ ceramic in terms of laser slope efficiency are superior to all previously studied $Tm^{3+}$-doped "mixed" sesquioxide ceramics and close to the best results for single-crystals.

The best result for the parent Tm:$Y_2O_3$ ceramic was achieved by Wang *et al.*: a diode-pumped $(Tm_{0.02}Y_{0.98})_2O_3$ laser generated 7.25 W at 2.05 μm with $\eta$ = 40% [13]. The slope efficiency achieved in this work with the Tm:$Y_2O_3$ ceramic is close to the best results reported for single-crystalline $Tm^{3+}$-doped sesquioxides [1,22].

To conclude, we report on highly-efficient ~2 μm laser operation of Tm:$Y_2O_3$ and Tm:$(Y,Sc)_2O_3$ transparent sesquioxide ceramics. For the both parent and solid-solution ceramics, the achieved laser slope efficiencies (70.2% and 44.7%) represent record-high values for any $Tm^{3+}$-doped sesquioxide ceramics being comparable with the best results for the corresponding single-crystals. It is due to an efficient cross-relaxation under high $Tm^{3+}$ doping level (5 at.%) and relatively low passive losses even for "mixed" compounds owing to an optimized synthesis procedure involving Tm:$(Y_{1-x}Sc_x)_2O_3$ laser-ablated nanoparticles with a mixture of cations at the atomic level and $ZrO_2$ as a grain growth inhibitor. The high thermal conductivity of ceramics paves the way towards power scaling under pumping by AlGaAs laser diodes at 0.8 μm or Raman-shifted Erbium fiber lasers at 1.68 μm (in-band pumping). The laser efficiency for "mixed" ceramics could be improved by reducing their residual porosity through optimization of the processing conditions and purification of the $Sc_2O_3$ raw powder. The solid-solution Tm:$(Y,Sc)_2O_3$ ceramics feature inhomogeneously broadened emission spectra extending up to 2.3 μm making them promising for sub-100 fs pulse generation from SESAM or Kerr-lens mode-locked lasers.

**Funding.** Agence Nationale de la Recherche (ANR-19-CE08-0028); Région Normandie (Chaire d'excellence "RELANCE"); Fonds Européen de Développement Régional (FEDER); Contrat de Plan État-Région (CPER) de Normandie; RFBR (21-53-15014); Ministry of Science and Higher Education of the Russian Federation (RF-2296.61321X0029, agreement 075-15-2021-687; Ural Federal University Program of Development Priority-2030).

**Acknowledgements.** The thermal properties were studied at the Center for Collective Use of the North-Caucasus Federal University.

**Disclosures.** The authors declare no conflicts of interest.

**Data availability.** Data underlying the results presented in this paper are not publicly available at this time but may be obtained from the authors upon reasonable request.

## References

1. P. Loiko, P. Koopmann, X. Mateos, J. M. Serres, V. Jambunathan, A. Lucianetti, T. Mocek, M. Aguiló, F. Díaz, U. Griebner, V. Petrov, and C. Kränkel, IEEE J. Sel. Top. Quantum Electron. **24**, 1600713 (2018).
2. K. van Dalfsen, S. Aravazhi, C. Grivas, S. M. García-Blanco, and M. Pollnau, Opt. Lett. **39**, 4380 (2014).
3. R. P. Leavitt, J. B. Gruber, N. C. Chang, and C. A. Morrison, J. Chem. Phys. **76**, 4775 (1982).
4. A. Suzuki, C. Kränkel, and M. Tokurakawa, Opt. Express **29**, 19465 (2021).
5. Y. Zhao, L. Wang, Y. Wang, J. Zhang, P. Liu, X. Xu, Y. Liu, D. Shen, J. E. Bae, T. G. Park, F. Rotermund, X. Mateos, P. Loiko, Z. Wang, X. Xu, J. Xu, M. Mero, U. Griebner, V. Petrov, and W. Chen, Opt. Lett. **45**, 459 (2020).
6. O. L. Antipov, A. A. Novikov, N. G. Zakharov, and A. P. Zinov'ev, Opt. Mater. Express **2**, 183 (2012).
7. O. Antipov, A. Novikov, S. Larin, and I. Obronov, Opt. Lett. **41**, 2298 (2016).
8. L. Fornasiero, E. Mix, V. Peters, K. Petermann, and G. Huber, Ceram. Int. **26**, 589 (2000).
9. J. Lu, J. F. Bisson, K. Takaichi, T. Uematsu, A. Shirakawa, M. Musha, K. Ueda, H. Yagi, T. Yanagitani, and A. A. Kaminskii, Appl. Phys. Lett. **83**, 1101 (2003).
10. J. Lu, K. Takaichi, T. Uematsu, A. Shirakawa, M. Musha, K. I. Ueda, H. Yagi, T. Yanagitani, and A. A. Kaminskii, Jpn. J. Appl. Phys. **41**, L1373 (2002).
11. Z. Zhou, X. Guan, X. Huang, B. Xu, H. Xu, Z. Cai, X. Xu, P. Liu, D. Li, J. Zhang, and J. Xu, Opt. Lett. **42**, 3781 (2017).
12. W. Jing, P. Loiko, J. Maria Serres, Y. Wang, E. Vilejshikova, M. Aguiló, F. Díaz, U. Griebner, H. Huang, V. Petrov, and X. Mateos, Opt. Mater. Express **7**, 4192 (2017).
13. H. Wang, H. Huang, P. Liu, L. Jin, D. Shen, J. Zhang, and D. Tang, Opt. Mater. Express **7**, 296 (2017).
14. Y. Wang, W. Jing, P. Loiko, Y. Zhao, H. Huang, X. Mateos, S. Suomalainen, A. Härkönen, M. Guina, U. Griebner, and V. Petrov, Opt. Express **26**, 10299 (2018).
15. V. V. Osipov, V. V. Platonov, V. V. Lisenkov, A. V. Podkin, and E. E. Zakharova, Phys. Status Solidi C **10**, 926 (2013).
16. P. Loiko, L. Basyrova, R. Maksimov, V. Shitov, M. Baranov, F. Starecki, X. Mateos, and P. Camy, J. Lumin. **240**, 118460 (2021).
17. L. Zhang, W. Pan, and J. Feng, J. Eur. Ceram. Soc. **35**, 2547 (2015).
18. R. Gaumé, B. Viana, D. Vivien, J. P. Roger, and D. Fournier, Appl. Phys. Lett. **83**, 1355 (2003).
19. J. A. Caird, S. A. Payne, P. Staber, A. Ramponi, L. Chase, and W. F. Krupke, IEEE J. Quantum Electron. **24**, 1077 (1988).
20. A. Suzuki, S. Kalusniak, H. Tanaka, M. Brützam, S. Ganschow, M. Tokurakawa, and C. Kränkel, Opt. Express **30**, 42762 (2022).
21. A. Pirri, R.N. Maksimov, V.A. Shitov, V.V. Osipov, E. Sani, B. Patrizi, M. Vannini, and G. Toci, J. Alloys Compd. **889**, 161585 (2021).
22. P. Koopmann, R. Peters, K. Petermann, and G. Huber, Appl. Phys. B **102**, 19 (2011).

## Full references


1. P. Loiko, P. Koopmann, X. Mateos, J. M. Serres, V. Jambunathan, A. Lucianetti, T. Mocek, M. Aguiló, F. Díaz, U. Griebner, V. Petrov, and C. Kränkel, "Highly-efficient, compact $Tm^{3+}$:$RE_2O_3$ (RE = Y, Lu, Sc) sesquioxide lasers based on thermal guiding," IEEE J. Sel. Top. Quantum Electron. **24**(5), 1600713-1-13 (2018).
2. K. van Dalfsen, S. Aravazhi, C. Grivas, S. M. García-Blanco, and M. Pollnau, "Thulium channel waveguide laser with 1.6 W of output power and ~80% slope efficiency," Opt. Lett. **39**(15), 4380-4383 (2014).
3. R. P. Leavitt, J. B. Gruber, N. C. Chang, and C. A. Morrison, "Optical spectra, energy levels, and crystal-field analysis of tripositive rare-earth ions in $Y_2O_3$. II. Non-Kramers ions in $C_2$ sites," J. Chem. Phys. **76**(10), 4775-4788 (1982).
4. A. Suzuki, C. Kränkel, and M. Tokurakawa, "Sub-6 optical-cycle Kerr-lens mode-locked Tm:$Lu_2O_3$ and Tm:$Sc_2O_3$ combined gain media laser at 2.1 µm," Opt. Express **29**(13), 19465-19471 (2021).
5. Y. Zhao, L. Wang, Y. Wang, J. Zhang, P. Liu, X. Xu, Y. Liu, D. Shen, J. E. Bae, T. G. Park, F. Rotermund, X. Mateos, P. Loiko, Z. Wang, X. Xu, J. Xu, M. Mero, U. Griebner, V. Petrov, and W. Chen, "SWCNT-SA mode-locked Tm:$LuYO_3$ ceramic laser delivering 8-optical-cycle pulses at 2.05 µm," Opt. Lett. **45**(2), 459-462 (2020).
6. O. L. Antipov, A. A. Novikov, N. G. Zakharov, and A. P. Zinov'ev, "Optical properties and efficient laser oscillation at 2066 nm of novel Tm:$Lu_2O_3$ ceramics," Opt. Mater. Express **2**(2), 183-189 (2012).
7. O. Antipov, A. Novikov, S. Larin, and I. Obronov, "Highly efficient 2 µm CW and Q-switched $Tm^{3+}$:$Lu_2O_3$ ceramics lasers in-band pumped by a Raman-shifted erbium fiber laser at 1670 nm," Opt. Lett. **41**(10), 2298-2301 (2016).
8. L. Fornasiero, E. Mix, V. Peters, K. Petermann, and G. Huber, "Czochralski growth and laser parameters of $RE^{3+}$-doped $Y_2O_3$ and $Sc_2O_3$," Ceram. Int. **26**(6), 589-592 (2000).
9. J. Lu, J. F. Bisson, K. Takaichi, T. Uematsu, A. Shirakawa, M. Musha, K. Ueda, H. Yagi, T. Yanagitani, and A. A. Kaminskii, "$Yb^{3+}$:$Sc_2O_3$ ceramic laser," Appl. Phys. Lett. **83**(6), 1101-1103 (2003).
10. J. Lu, K. Takaichi, T. Uematsu, A. Shirakawa, M. Musha, K. I. Ueda, H. Yagi, T. Yanagitani, and A. A. Kaminskii, "$Yb^{3+}$:$Y_2O_3$ ceramics – a novel solid-state laser material," Jpn. J. Appl. Phys. **41**(12A), L1373-L1375 (2002).
11. Z. Zhou, X. Guan, X. Huang, B. Xu, H. Xu, Z. Cai, X. Xu, P. Liu, D. Li, J. Zhang, and J. Xu, "$Tm^{3+}$-doped $LuYO_3$ mixed sesquioxide ceramic laser: effective 2.05 µm source operating in continuous-wave and passive Q-switching regimes," Opt. Lett. **42**(19), 3781-3784 (2017).
12. W. Jing, P. Loiko, J. Maria Serres, Y. Wang, E. Vilejshikova, M. Aguiló, F. Díaz, U. Griebner, H. Huang, V. Petrov, and X. Mateos, "Synthesis, spectroscopy, and efficient laser operation of "mixed" sesquioxide Tm:$(Lu,Sc)_2O_3$ transparent ceramics," Opt. Mater. Express **7**(11), 4192-4202 (2017).
13. H. Wang, H. Huang, P. Liu, L. Jin, D. Shen, J. Zhang, and D. Tang, "Diode-pumped continuous-wave and Q-switched Tm:$Y_2O_3$ ceramic laser around 2050 nm," Opt. Mater. Express **7**(2), 296-303 (2017).
14. Y. Wang, W. Jing, P. Loiko, Y. Zhao, H. Huang, X. Mateos, S. Suomalainen, A. Härkönen, M. Guina, U. Griebner, and V. Petrov, "Sub-10 optical-cycle passively mode-locked Tm:$(Lu_{2/3}Sc_{1/3})_2O_3$ ceramic laser at 2 µm," Opt. Express **26**(8), 10299-10304 (2018).
15. V. V. Osipov, V. V. Platonov, V. V. Lisenkov, A. V. Podkin, and E. E. Zakharova, "Production of nanopowders of oxides by means of fiber and pulse-periodical $CO_2$ lasers," Phys. Status Solidi C **10**(6), 926-932 (2013).
16. P. Loiko, L. Basyrova, R. Maksimov, V. Shitov, M. Baranov, F. Starecki, X. Mateos, and P. Camy, "Comparative study of Ho:$Y_2O_3$ and Ho:$Y_3Al_5O_{12}$ transparent ceramics produced from laser-ablated nanoparticles," J. Lumin. **240**, 118460-1-22 (2021).
17. L. Zhang, W. Pan, and J. Feng, "Dependence of spectroscopic and thermal properties on concentration and temperature for Yb:$Y_2O_3$ transparent ceramics," J. Eur. Ceram. Soc. **35**(9), 2547-2554 (2015).
18. R. Gaumé, B. Viana, D. Vivien, J. P. Roger, and D. Fournier, "A simple model for the prediction of thermal conductivity in pure and doped insulating crystals," Appl. Phys. Lett. **83**(7), 1355-1357 (2003).
19. J. A. Caird, S. A. Payne, P. Staber, A. Ramponi, L. Chase, and W. F. Krupke, "Quantum electronic-properties of the $Na_3Ga_2Li_3F_{12}$:$Cr^{3+}$ laser," IEEE J. Quantum Electron. **24**(6), 1077-1099 (1988).
20. A. Suzuki, S. Kalusniak, H. Tanaka, M. Brützam, S. Ganschow, M. Tokurakawa, and C. Kränkel, "Spectroscopy and 2.1 µm laser operation of Czochralski-grown $Tm^{3+}$:$YScO_3$ crystals," Opt. Express **30**(23), 42762-42771 (2022).
21. A. Pirri, R.N. Maksimov, V.A. Shitov, V.V. Osipov, E. Sani, B. Patrizi, M. Vannini, and G. Toci, "Continuously tuned $(Tm_{0.05}Sc_{0.252}Y_{0.698})_2O_3$ ceramic laser with emission peak at 2076 nm," J. Alloys Compd. **889**, 161585 (2021).
22. P. Koopmann, R. Peters, K. Petermann, and G. Huber, "Crystal growth, spectroscopy, and highly efficient laser operation of thulium-doped $Lu_2O_3$ around 2 µm," Appl. Phys. B **102**(1), 19-24 (2011).